Composites Science and Technology 129 (2016) 101–107

Contents lists available at ScienceDirect

Composites Science and Technology

journal homepage: http://www.elsevier.com/locate/compscitech

Partially sulfonated Poly(arylene ether sulfone)/organically modified metal oxide nanoparticle composite membranes for proton exchange membrane for direct methanol fuel cell

Wonmok Lee [a, *], Seung Chul Gil [a], Haekyoung Kim [b], Kyusung Han [c], Hyunjung Lee [d]

[a] Department of Chemistry, Sejong University, 98 Gunja-dong, Gwangjin-gu, Seoul, 143-747, South Korea
[b] School of Materials Science and Engineering, Yeungnam University, Gyeongsangbuk-do, 712-749, Republic of Korea
[c] Korea Institute of Ceramic Engineering and Technology, Icheon, Gyeonggi, 467-843, Republic of Korea
[d] School of Advanced Materials Engineering, Kookmin University, 861-1 Jeongneung-dong, Seoul, 136-702, South Korea

ARTICLE INFO

Article history:
Received 6 November 2015
Received in revised form
10 April 2016
Accepted 14 April 2016
Available online 24 April 2016

Keywords:
Direct methanol fuel cell
Poly(arylene ether sulfone)
Composite membrane
Metal oxide nanoparticle
Mechanical property

ABSTRACT

Organic/inorganic composite proton exchange membranes (PEMs) of sulfonated poly(arylene ether sulfone) (sPSF) and organically modified metal oxide nanoparticles are demonstrated. The sPSF ionomers with three different degree of sulfonations (DS) (39, 42, 48%) were synthesized by condensation polymerization, and nanocrystalline titania and zirconia particles were respectively prepared by sol–gel reactions catalyzed by p-toluene sulfonic acid (PTSA) in the presence of acetylacetone (AcAc) as an organic surface modifier. Through structural analyses, non-aggregated anatase titania with ~7 nm average size and tetragonal zirconia with ~4 nm size were confirmed. The transparent composite membranes with 1 wt% nanoparticle contents were obtained by simply mixing sPSF and the respective nanoparticles in dimethylsulfoxide (DMSO) followed by membrane casting. Post-treatment in aqueous sulfuric acid resulted in the composite membranes exhibiting reduced proton conductivities and highly improved methanol permeabilities and water uptakes compared to the prestine sPSF membranes. Overall, the zirconia-containing sPSF (with 48% DS) composite membrane exhibited the best PEM property and an active mode DMFC performance tests on the membrane-electrode assemblies (MEA) with various PEMs also revealed that the zirconia nanocomposite membrane exhibits the best power density. The maximum power density from zirconia/sPSF48 composite MEA was measured to be 73 mW/cm^2 at 60 °C with 1 M methanol fuel which is 7% higher than that of Nafion-115 MEA. The improved PEM properties of the composite membranes developed in this study can be attributed to the effective barrier effect of both titania and zirconia nanoparticles provided by their small particle sizes (<10 nm) without significant aggregation within the sPSF matrix, and also to the hydrophilic nanoparticle surfaces to enable the improved water retaining properties for the composited PEM.

© 2016 Published by Elsevier Ltd.

1. Introduction

Recently, there are ongoing researches on eco-friendly renewable energy devices such as fuel cells and solar cells to make up the conventional energy sources which consume the limited resources [1]. Among them, fuel cells exhibit high energy efficiency as well as high power density for electrical energy conversion, and many different types of fuel cells are available depending on the demanded power for the devices. Direct methanol fuel cell (DMFC) is gathering particular interest as a promising energy source for the small mobile devices such as cellular phone and radio frequency identification (RFID) due to its advantageous features such as easy fuel storage, low operating temperature and simple device design capability [2,3]. Toward stable generation of electricity in DMFC, there are several prerequisite requirements among which facile and selective proton transport through the proton exchange membrane (PEM) is one of the most important demands. Nafion has been most popular PEM for DMFC so far due to high proton conductivity, chemical/mechanical stability, and excellent processability for fabricating membrane electrode assembly (MEA), while some of the critical disadvantages such as high methanol crossover and high manufacturing cost still limit its practical application for the

* Corresponding author.
E-mail address: wonmoklee@sejong.ac.kr (W. Lee).

http://dx.doi.org/10.1016/j.compscitech.2016.04.020
0266-3538/© 2016 Published by Elsevier Ltd.

DMFC devices [2,4–6]. Therefore, efforts have been devoted to develop alternative PEMs by sulfonating the hydrocarbon based engineering plastics such as poly(styrene) (PS) [7], PS-based block copolymers [8–10], poly(arylene ether ether ketone) [11,12], poly(imide) [13], poly(phosphazene) [14], poly(arylene ether sulfone) (PSF) [15–17] which exhibit low methanol permeability and cost effectiveness. In addition to the developments of ionomer synthesis, incorporation of inorganic nanoparticles into the PEM materials have also drawn researchers' attention since the nanocomposite membrane is capable of further reduction of methanol crossover via barrier effect of well-dispersed nanoparticles and an improved water-retaining property due to the hydrophilic nature of inorganic particles [18,19]. Various nano-sized hydrophilic inorganic fillers have been adopted for the fabrication of organic-inorganic nanocomposite PEM such as silica [20,21], titania [19,22], zirconia [23,24], zeolite [25], and montmorillonite [26–29].

Although the hybrid nanocomposite PEMs listed above generally showed improved PEM properties and DMFC performances as well, one of the most challenging issues are maintaining uniform dispersion of nanoparticles within PEM after film casting. Due to entropic driving force, mixing the particulate materials with the high molecular weight polymers is quite unfavorable, and therefore the nanoparticles tend to form large aggregates (>1 μm) during solvent removal even though their surface is chemically treated to resemble the ionic functional groups of the ionomer to be blended [26]. In addition, the original particle size and size distribution of the inorganic nanoparticles are limited, although the small and uniform particle size is strongly required to achieve better performances of the composite membranes. Existence of large aggregates of inorganic nanoparticles in a composite membrane not only reduce the barrier effect for methanol crossover, but also deteriorate the mechanical integrity of the membrane to result in crack formation.

Recently, we have reported the preparation of the organically modified nano-crystalline titania which exhibits uniform size (~5 nm) and excellent dispersibility in alcoholic media [30]. In spite of high crystallinity and refractive index of titania nanoparticle, a completely transparent thin film could be obtained as well as a liquid dispersion in organic solvent evidently showing negligible aggregations in both states. Such an excellent dispersibility was provided by acetylacetone (AcAc) ligand surrounding the surface of titania nanoparticle via stable coordination bond with terminal Ti atom [31].

In this study, we applied the similar synthetic procedure for titania to the preparation of nano-crystalline zirconia, and investigated the hybridization of titania and zirconia with tailor-made sPSF ionomers toward PEM application for DMFC.

2. Experimental methods

2.1. Materials

N-methyl-2-pyrrolidone (NMP), dimethylsulfoxide (DMSO), toluene, potassium carbonate, fuming sulfuric acid (30%), allyl chloride, and propargyl bromide were purchased from sigma Aldrich. Isopropyl alchol, n-hexane, methanol, dimethylacetamide (DMAc), acetone were purchased from Samjun. 4,4-dichlorodiphenylsulfone (DCDPS), Bisphenol-A (BPA), chlorobenzene, and tetrabutylammonium hydrogen sulfate (TBAHS) were purchased from TCI. BPA and DCDPS were purified by recrystallization from toluene and methanol respectively. Sulfonated DCDPS was prepared by reacting DCDPS with fuming sulfuric acid and subsequent recrystallization [17]. For DMFC performance test, platinum (Pt, HIGHSPEC 13100) black powder and platinum-ruthenium (Pt–Ru, HIGHSPEC 12100) alloy powder were obtained from Johnson-Matthey, and Nafion® dispersion (10 wt%, Equivalent weight 1100) was purchased from Dupont. Deionized (DI) water was prepared by water purification system (Humantech).

2.2. Synthesis of Poly(arylene ether sulfone)

Linear sPSFs with terminal hydroxyl group was synthesized by condensation polymerization using DCDPS, 3,3′-disulfonated-4,4′-dichlorodiphenyl sulfone (SDCDPS), and BPA as respective monomers [17]. The polymers with three different degrees of sulfonation (DS) were obtained by controlling mixing ratios of DCDPS and SDCDPS. Typical polymerization procedures are as follows. BPA 0.02 mol, K_2CO_3 11.04 g, DCDPS xmol, and SDCDPS y mol($x + y = 0.02$ mol) were added to 250 mL round bottomed flask (RBF) immersed in oil bath after nitrogen purging for 1 h 60 mL of anhydrous NMP and 30 mL toluene were added as a solvent and an azeotropic agent respectively. After flowing nitrogen for 1 h with stirring, the bath temperature is increased to 160 °C for 90 min, at which azeotropic mixture of toluene and water was collected at Dean-stark trap. Temperature was further elevated to 230 °C and polymerization reaction proceeded for 3–4 h under nitrogen environment. The reaction scheme is shown in Scheme 1. The reaction mixture was cooled down to room temperature, and precipitated in 1 L IPA under vigorous stirring. The product was filtered and dried at 70 °C in an oven. The remaining salt within the product was washed with water three times, and the purified product was finally dried at 70 °C [16].

2.3. Synthesis of titania and zirconia nanoparticles

Organically modified nanoparticles of titania and zirconia were synthesized by sol–gel process [30]. 1 mol 1-butanol, 0.1 mol AcAc, and 0.1 mol $Ti(Obu)_4$ (or $Zr(Obu)_4$) were added to 250 mL RBF and mixed by magnetic stirring for 15 min. 0.02 mol p-toluene sulfonic acid was dissolved in 18 mL of DI water in ice bath, and slowly added to the reaction mixture using a syringe. The sol–gel reaction proceeded at 60 °C for 24 h, and the product was precipitated in 1 L toluene. The precipitated product was redispersed in 1-butanol, precipitated in toluene, centrifuged at 1500 rpm, and the liquid is decanted. The purified nanoparticle was vacuum-dried at room temperature [30].

2.4. Fabrication of composite membranes

The composite membranes of sPSF and inorganic nanoparticles were prepared by solution casting method. First, 5 wt% of a polymer solution in DMSO was filtered through 1 μm disk filter (Whatman). Then this solution was mixed with 1 wt% of nanoparticle dispersion in DMSO so that the polymer/nanoparticle ratio becomes 100/1 by weight. The mixed solution was stirred at 80 °C for 24 h, and poured to a glass petri dish (diameter = 10 cm) in a casting chamber. The composite membrane was cast at 60 °C for 24 h under nitrogen flow which was followed by annealing at 120 °C for 2 h in a vacuum oven. After complete drying, the membrane thicknesses were measured to be ~100 μm. The dried membrane was soaked in 5 wt% aqueous sulfuric acid at 50 °C for 48 h, and rinsed with DI water several time to remove remaining acid from the PEM.

2.5. Characterizations

For determination of DS in sPSF, an ionomer was dissolved in deuterated DMSO (DMSO-D_6), and 1H NMR spectrum was obtained using Bruker spectrometer (500 Mhz). DS of sPSF was calculated by comparing proton signals from DCDPS and SDCDPS. Average molecular weight of sPSF was measured using gel permeation

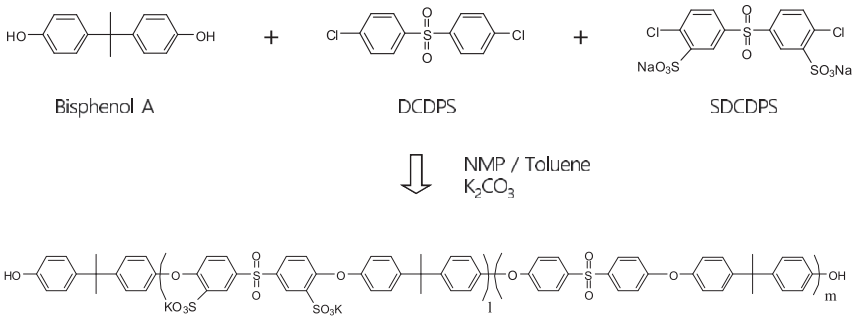

Scheme 1. Condensation polymerization of partially sulfonated poly(arylene ether sulfone).

chromatography (GPC, Younglin LC System) using DMF (with 0.2 wt % LiBr) as solvent, and the results are summarized in Supplementary data S-1. Crystal structure of titania and zirconia nanoparticles were characterized by X-ray diffraction (XRD, Rigaku D/Max-2500) using Cu-Kα radiation as light source within 2theta range of 20°–80°. Dispersion of the nanoparticles in sPSF PEM was analyzed by transmission electron microscopy (TEM). One drop of 10-fold diluted solution of sPSF48 containing each nanoparticle in DMSO was placed on a Cu grid, and it was dried at 60 °C for 24 h and 120 °C for 24 h respectively to follow the same thermal history to that of the membrane casting. The dried sample was imaged by high TEM (Tecnai F20 FEI) [32]. For water uptake measurement of PEM, a 1 × 1cm^2 membrane was soaked in DI water at 30 °C for 24 h. After wiping out excess water at the PEM surface, a wet PEM was quickly weighed, and it was dried at 80 °C for 24 h after which a dried PEM was weighed to give the water uptake value $((W_{wet} - W_{dried})/W_{dried})$ [15]. Proton conductivity of a PEM was measured by four-point probe method using an impedance analyzer (IVIUM, COMPACTSTAT). After hydrating a PEM in DI water for 24 h, it was fixed on a custom-made conductivity cell and Nyquist plot was obtained at 30 °C. Proton conductivity was calculated by using an equation; $\sigma = L/(A \times R)$, where σ is proton conductivity, L is a distance between electrodes, and R is resistance of the PEM [33]. Methanol permeability of a PEM was measured using a custom-made plastic cell which is composed of two 35 mL chambers (V_A and V_B) between a PEM having 2 × 2cm^2 area for methanol transport. V_A and V_B were filled with DI water and 3 M methanol respectively, and time-dependent concentration variation in V_A (C_A) was measured using a refractrometer (Atago, RX-5000a, Japan). Calculation of methanol permeability was carried out by using an equation; $C_A(t) = C_B(A/L)(DK/V_B)(t - t_0)$, where C is methanol concentration, A and L are an area and a thickness of the membrane, D and K are methanol diffusivity and distribution coefficient, and t and t_0 are the time for each measurement and starting time respectively. DK stands for methanol permeability [34].

2.6. MEA fabrication and DMFC performance test

Using each composite membrane, a DMFC MEA was fabricated by following procedures. A dried PEM was sandwiched between anode (4.17 mg/cm^2 Pt–Ru loaded on Toray 060 carbon paper) and cathode (2.78 mg cm^2 Pt loaded on SGL 25BC) where each catalyst was mixed with 20 wt% Nafion binder, and hot-pressed for 1 min at 80 °C and 5 MPa pressure. The MEA was assembled to a single cell, activated by flowing 1 M methanol for 1day, and active mode DMFC test was performed using 1 M methanol anode fuel at 3 mL/min flow rate and 400 mL/min air flow at the cathode at the temperature range between 30 °C–60 °C. For comparison, an MEA with Nafion 115 PEM was fabricated by hot-pressing for 1 min at 150 °C and 5 MPa, and DMFC single cell test was performed at the same condition as used for the composite PEM [26].

3. Results and discussion

We followed the synthetic method as reported by McGrath and coworkers to prepare three highly sulfonated PSF ionomers respectively with 39, 42, 48% DS by controlling molar ratios of DCDPS and SDCDPS monomers during the condensation polymerization [15]. DS of each sPSF was calculated from the proton signals of 1H NMR (500 MHz Bruker). Based on the DS values obtained, the sPSF samples were named as sPSF39, sPSF42, and sPSF48 respectively. All of sPSF ionomers formed tough membranes by solution casting owing to the high molecular weights. The molecular weights of sPSF39, sPSF42, and sPSF48 were measured to be 189 kDa, 129 kDa, and 219 kDa respectively. Organically modified titania and zirconia nanoparticles were synthesized via sol–gel route. Although we have previously reported the preparation and utilization of organically modified titania nanoparticles [30,35,36], this is the first report on the nanocrystalline zirconia synthesis using AcAc ligand and PTSA catalyst. Both titania and zirconia nanoparticles were obtained as white powders, and their crystalline structures and average particle sizes were characterized by XRD analysis. As shown in Fig. 1(a), the titania particles exhibited a typical diffraction peaks of anatase phase, and Scherer analysis on {101} peak revealed that the particle size was 7 nm [30]. Zirconia nanoparticles showed relatively broader diffraction peaks than those of titania owing to its smaller average particle size which was calculated to be ~4 nm from the first diffraction peak. Two major peaks appeared at 25–30° and 55–60° which were respectively assigned to be from {111} and {220},{311} planes of tetragonal zirconia crystalline phase [37]. Owing to a broadness of the diffraction signal, the peaks from tetragonal {220} and {311} planes of zirconia nanoparticle were not resolved. The small particle sizes of titania and zirconia could be obtained by controlling PTSA catalyst amounts [30].

With the same PTSA added to the respective sol–gel reactions, different particle sizes of titania and zirconia could be attributed to the distinct hydrolysis-condensation kinetics of $Ti(Obu)_4$ and $Zr(Obu)_4$ precursors. Both nanoparticles were readily dispersed in polar organic solvents including 1-butanol and DMSO, where DMSO is the solvent for sPSF. We tested the mixing of titania and zirconia dispersions with sPSF solution to have various nanoparticle contents in the solution-cast composite membranes, and it was found that the transparent membranes could be obtained with the nanoparticle contents up to 1 wt% for both cases. The composite membranes containing more than 1 wt% of nanoparticles exhibited visible opaqueness which implies aggregate formation. Therefore, nanoparticle content was fixed to 1 wt% with respect to polymer for the preparation of every composite PEM. In order to confirm the

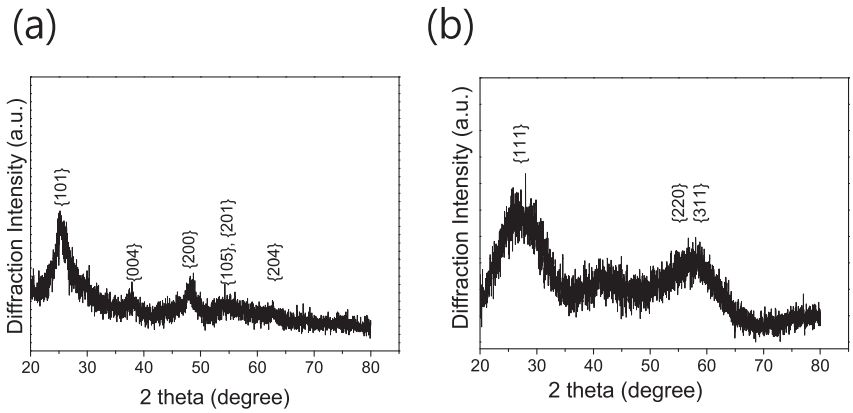

Fig. 1. XRD Results of (a) titania, (b) zirconia nanoparticles, respectively showing anatase and tetragonal crystalline structures.

nanoparticle dispersibilities in sPSF membranes, TEM analysis on the composite membranes containing 1 wt% nanoparticles was carried out. For TEM analysis, one drop of the 10-fold diluted sPSF48/nanoparticle solution used for PEM preparation was cast onto a Cu grid so that a very thin PEM film can be formed. As shown in Fig. 2, both titania and zirconia nanoparticles are well dispersed in sPSF matrices without significant aggregations.

Titania nanoparticle showed a relatively larger size and broader size distribution compared to zirconia which is in a good accordance to the XRD analysis results. The inset photographs in Fig. 2(a) and (b) are the composite membranes of sPSF with titania and zirconia respectively. Both membranes were cast to 100 μm thicknesses to be used for actual PEM for DMFC. It is noteworthy that the both membranes are transparent enough to be seen through although the 1 wt% of highly crystalline inorganic nanoparticles are included. Such outstanding dispersions of titania and zirconia within polymeric matrix could be attributed to the surface modification by AcAc ligand which effectively improved compatibilities between nanoparticles and sPSF matrix as schematically shown in Fig. 3. Tensile stress measurements of the hydrated PEMs of sPSF-48 and its composite membranes revealed that the 1 wt% zirconia-containing sPSF-48 shows ~30% improvement of tensile stress at low strain (5%) regime compared to a pristine membrane implying the reinforced mechanical strength was achieved owing to a successful hybridization of inorganic filler with PEM material. (see supplementary data S-2).

Using the composite membranes, various PEM characterizations were performed. The six composite PEMs were prepared by respectively blending titania and zirconia nanoparticles with three different sPSF's (*i.e.* sPSF39, sPSF42, sPSF48 by DS) at 1 wt%. For instance, sPSF39-T1 (or sPSF39-Z1) stands for the composite membrane of sPSF39 and 1 wt% organically modified titania nanoparticle (or the same content of zirconia). Each sPSF membrane without nanoparticle was also prepared for comparison. In Table 1, the characterization results of nine PEMs are summarized along with those of Nafion-115. As shown in Table 1 and Fig. 4(a) and(b), proton conductivities and water uptake results of three sPSF membranes were measured at 30 °C, both of which evidently showed an increasing tendencies as a function of DS due to higher content of hydrophilic domains in PEM [8]. The proton conductivity of a sPSF48 membrane was measured to be as high as 0.08S/cm which is comparable to that of Nafion-115. Upon inclusion of 1 wt% organically modified nanoparticles, the proton conductivities of the composite membranes decreased by 10–20%.

Decrease in proton conductivity was less serious for the zirconia composite membranes, presumably due to a smaller particle size and more uniform size distribution of the zirconia nanoparticle compared to those of the titania used in this study.

For usual organic/inorganic composite PEMs, reduction of the proton conductivity compared to that of a PEM without inorganic nanoparticle is commonly observed since the inorganic fillers tend to block the hydrophilic channels for proton transportation

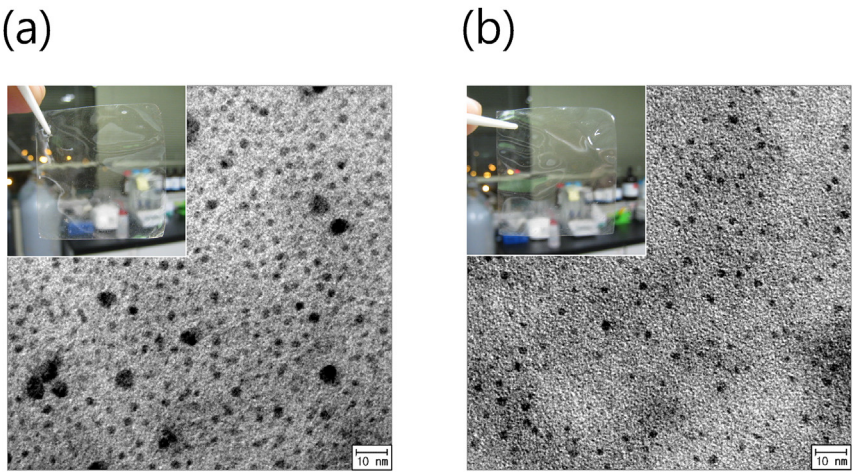

Fig. 2. TEM micrographs of (a) titania, (b) zirconia dispersed in sPSF48 at 1 wt%. Inset figures respectively show the corresponding composite membranes with 100 μm thicknesses.

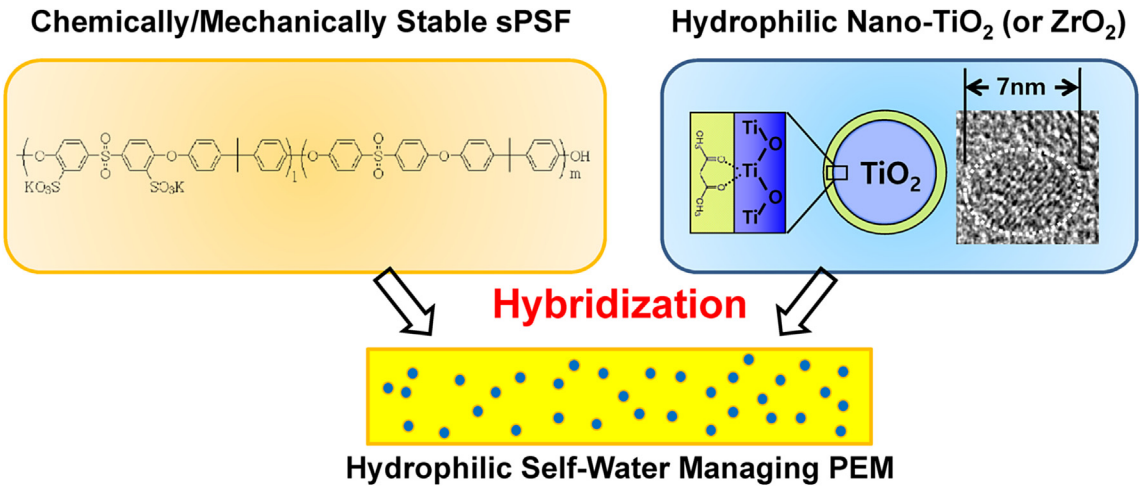

Fig. 3. Schematic illustration of hybrid PEM of sPSF and well-dispersed nano-titania (or zirconia) due to an improved compatibility. The imbedded transmission electron microscopy image of a titania nanoparticle shows anatase crystalline structure.

Table 1
Characterization results of PEM.

Sample	Proton conductivity[a] (S/cm)	Methanol permeability[a] (cm^2/s)	Water uptake[a] (wt%)	Selectivity (normalized to Nafion-115)
Nafion-115	0.078	2.7×10^{-6}	26.7	1.0
sPSF39	0.066	6.7×10^{-7}	55.7	3.4
sPSF39-T1	0.053	6.4×10^{-7}	62.1	2.9
sPSF39-Z1	0.059	7.1×10^{-7}	64.3	2.9
sPSF42	0.075	8.5×10^{-7}	59.8	3.1
sPSF42-T1	0.064	7.4×10^{-7}	67.8	3.0
sPSF42-Z1	0.071	7.5×10^{-7}	67.9	3.3
sPSF48	0.08	1.6×10^{-6}	65.6	1.7
sPSF48-T1	0.072	1.1×10^{-6}	71.6	2.3
sPSF48-Z1	0.077	1.1×10^{-6}	72.0	2.4

[a] All the measurements were carried out at 30 °C.

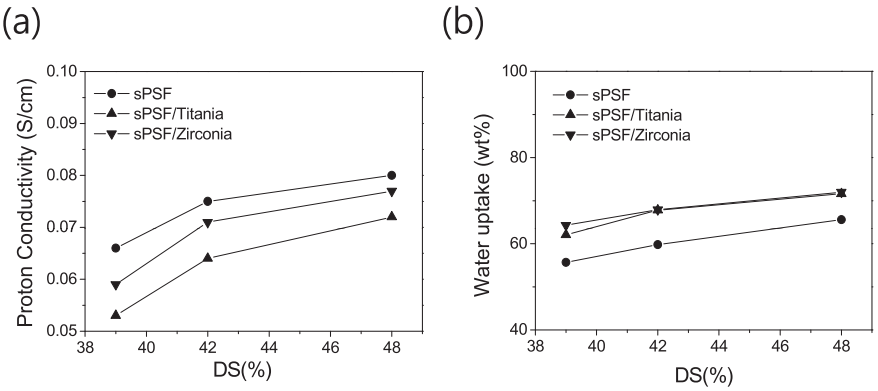

Fig. 4. (a) Proton conductivities, and (b) Water uptake results of sPSFs and nanocomposite membranes as a function of DS.

[24,38,39].

In order to minimize such behaviors and to provide a facile proton conduction, the surfaces of inorganic fillers are often modified with sulfate or sulfonate which resemble ionic functional groups in PEM materials [24,40]. In the current investigation, however, the surface modifier was non-ionizable AcAc. Nevertheless, only 10% reduction of proton conductivity was obtained for a sPSF/zirconia composite membrane which is quite noteworthy. Another evidence for indication of hydrophilic property of the PEM was found from the water uptake measurement. In Fig. 4(b), water uptake results of sPSF and the composite membranes are plotted against DS which evidently show the improved water uptake for both titania and zirconia composite membranes. Inclusion of sulfated metal oxide nanoparticles within PEM materials are regarded to improve water uptake property at room temperature and elevated temperatures [24,39]. Although our nanoparticle surfaces were initially stabilized by AcAc organic modifier which provided outstanding dispersability in polymer matrices during PEM casting, the surface groups of the embedded nanoparticles should have been exchanged by sulfate groups upon post-membrane treatment in aqueous sulfuric acid following the same mechanism as reported elsewhere [24]. Supposed that, the

composite membranes containing surface-treated nanoparticles would have become hydrophilic enough to provide an improved water retaining-property and high proton conductivity as experimentally verified in this study.

The most important role of the nanoparticle in the composite membrane is a reduction of methanol permeability by "barrier effect". In Fig. 5(a), methanol permeability of sPSF and the composite membranes are plotted. In general, a hydrocarbon PEM with high DS exhibits a trade-off phenomenon of high proton conductivity and methanol permeability as well. Our sPSF showed the same trends in both properties with increased DS, where the reduction of the methanol permeability in both composite membranes was more substantial at higher DS's. Composite membranes of metal oxide nanoparticles with PEM material often show reduction of methanol permeability. Hasani-Sadrabadi et al. reported that an electro-osmotic movement of methanol takes place in DMFC similarly as water transport, and their diffusion path become complicated owing to the presence of well-dispersed nanoparticles resulting in reduced permeability [29].

We calculated the membrane selectivities of the PEMs used in this study by dividing proton conductivities by methanol permeabilities, and then normalized the selectivities to the value of Nafion-115 as listed in Table 1 for easier comparison. For sPSF membranes without nanoparticles, the membrane selectivities of sPSF39, sPSF42, and sPSF48 were calculated to be 3.4, 3.1 and 1.7 respectively due to more substantial increase of methanol permeabilities in the PEM of higher DS. Fig. 5(b) shows a quite interesting tendency of the membrane selectivity as a function of DS.

Although incorporation of the metal oxide nanoparticles within sPSF39 did not improve the membrane selectivity, both nanocomposites using sPSF48 exhibited noticeable increases in the membrane selectivity. These results imply that the barrier effects of our titania and zirconia nanoparticles are more effective in the highly sulfonated PEMs. We also examined proton conductivities and membrane selectivities of the composite PEMs of sPSF48 containing 0,1,3,5 wt% of each nanoparticle as shown in Supplementary data S-3, and confirmed that 1 wt% composite PEM showed the best selectivity.

Using the sPSF48 PEM and its nanocomposite PEMs respectively, DMFC MEAs were fabricated, and active mode single cell performance tests were carried out as shown in Fig. 6. For comparison, an MEA test with Nafion-115 PEM was also conducted.

At 60 °C, an MEA with sPSF48 MEA exhibited the maximum power density of 63 mW/cm^2, which was found to be ~7% lower than that with Nafion-115 (68 mW/cm^2). An MEA with sPSF48-T1 showed 69 mW/cm^2 which is comparable or slightly higher than that of Nafion-115 PEM. The best MEA performance was achieved from sPSF48-Z1 PEM, which was 73 mW/cm^2 (7% higher than with Nafion-115). The improvements in power density from both titania and zirconia nanocomposite PEMs can be attributed to the effective reduction of methanol permeability and enhanced water retaining ability by well-dispersed hydrophilic nanoparticles within sPSF48 without significant loss of proton conductivities. Since the proton conductivity of sPSF48-Z1 was even higher than Nafion-115, we were able to get a 7% improved DMFC performance [20]. Taking into account that we actually adopted the MEA fabrication procedure optimized for Nafion PEM, higher power performances with a hydrocarbon-based nanocomposite PEMs are worthwhile to note. We expect that optimizations of MEA fabrication process for sPSF-based PEMs and development of a binder material that is better compatible with sPSF PEM would promise further improvement of DMFC performance with the PEM materials developed in this study.

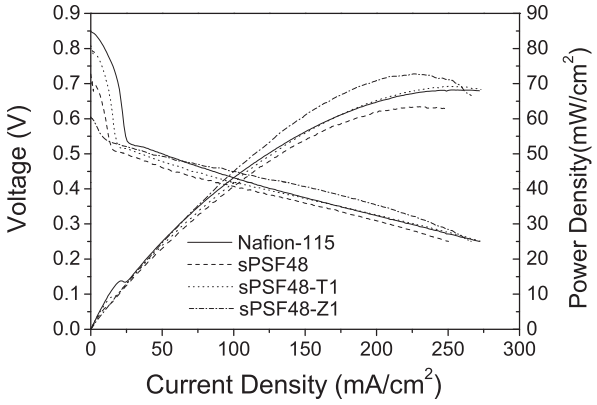

Fig. 6. DMFC power performance curves of MEAs containing different PEMs at 60 °C. All measurements were performed after activating each MEA with 1 M methanol for 1day.

4. Conclusions

For DMFC PEM application, we developed highly dispersed metal oxide nanoparticle composite membranes of sPSF ionomers with 39, 42, 48% of respective DS's which were synthesized by electrophilic aromatic polycondensation. Organically modified nanocrystalline titania and zirconia nanoparticles were synthesized through sol–gel reaction, and outstanding dispersion of both nanoparticles within ionomeric PSF were possible due to small particle sizes (<10 nm) and organic modification of nanoparticle surfaces by AcAc ligand. Inclusion of metal oxide nanoparticles resulted in slight reduction of proton conductivity in sPSF composite membranes, but the water uptake of the membrane was significantly increased due to hydrophilicity of the nanoparticles. Owing to the effective barrier effects provided by highly dispersed

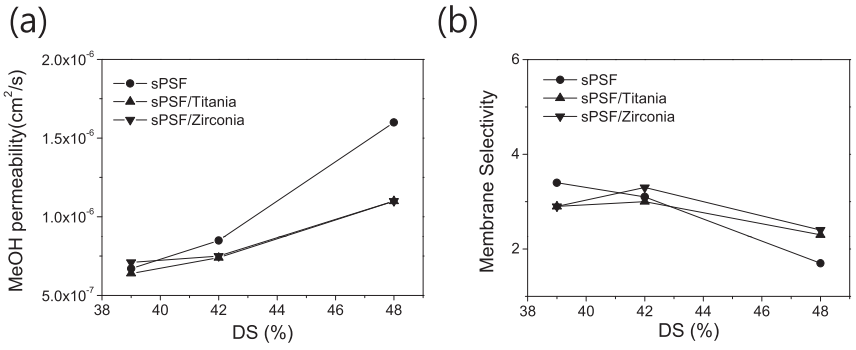

Fig. 5. (a) Methanol permeabilities and (b) Normalized membrane selectivities of sPSFs and nanocomposite membranes as a function of DS.

nanoparticles, methanol permeabilities of the composite membranes were improved particularly for the sPSF of high DS (PSF48). Overall, zirconia-containing sPSF PEM showed the highest membrane selectivity among other PEMs probably due to smaller particle size and more uniform size distribution compared to those of titania as revealed by TEM. Active mode DMFC performance tests were conducted for the respective MEAs with PSF48 and its nanocomposite PEMs, and the results were compared to that of a Nafion-115 MEA at the same condition. A single cell with Nafion 115 exhibited the maximum power density of 68 mW/cm^2 at 60 °C, while those with sPSF48-T1 and sPSP48-Z1 resulted in the improved performances of 69 mW/cm^2, and 73 mW/cm^2 respectively.

Acknowledgments

This paper was written to the memory of Dr. S. Lim who had worked for Korea Institute of Energy Research. Authors also thank Dr. D-H. Jung for allowing us to use the fuel cell test facilities. This study was financially supported by Basic Science Research Program through the National Research Foundation of Korea funded by the Ministry of Education, Science and Technology (2013R1A1A2011168).

Appendix A. Supplementary data

Supplementary data related to this article can be found at http://dx.doi.org/10.1016/j.compscitech.2016.04.020.

References

[1] K. Sopian, W.R. Wan Daud, Challenges and future developments in proton exchange membrane fuel cells, Renew. Energy 31 (5) (2006) 719–727.
[2] A. Kuver, W. Vielstich, Investigation of methanol crossover and single electrode performance during DMFC operation: a study using a solid polymer electrolyte membrane fuel cell system, J. Power Sources 74 (2) (1998) 211–218.
[3] T. Schultz, S. Zhou, K. Sundmacher, Current status of and recent developments in the direct methanol fuel cell, Chem. Eng. Tech. 24 (12) (2001) 1223–1233.
[4] S.R. Narayanan, A. Kindler, B. Jeffries-Nakamura, W. Chun, H. Frank, M. Smart, et al., Recent advances in PEM liquid-feed direct methanol fuel cells, in: Battery Conference on Applications and Advances, 1996, Eleventh Annual, 1996, pp. 113–122.
[5] V. Neburchilov, J. Martin, H.J. Wang, J.J. Zhang, A review of polymer electrolyte membranes for direct methanol fuel cells, J. Power Sources 169 (2) (2007) 221–238.
[6] S.H. Tian, D. Shu, Y.L. Chen, M. Xiao, Y.Z. Meng, Preparation and properties of novel sulfonated poly(phthalazinone ether ketone) based PEM for PEM fuel cell application, J. Power Sources 158 (1) (2006) 88–93.
[7] B. Smitha, S. Sridhar, A.A. Khan, Synthesis and characterization of proton conducting polymer membranes for fuel cells, J. Membr. Sci. 225 (1–2) (2003) 63–76.
[8] W. Lee, H. Kim, H. Lee, Proton exchange membrane using partially sulfonated polystyrene-b-poly (dimethylsiloxane) for direct methanol fuel cell, J. Membr. Sci. 320 (1–2) (2008) 78–85.
[9] J. Won, H.H. Park, Y.J. Kim, S.W. Choi, H.Y. Ha, I.H. Oh, et al., Fixation of nanosized proton transport channels in membranes, Macromolecules 36 (9) (2003) 3228–3234.
[10] Y.A. Elabd, E. Napadensky, J.M. Sloan, D.M. Crawford, C.W. Walker, Triblock copolymer ionomer membranes part I. methanol and proton transport, J. Membr. Sci. 217 (1–2) (2003) 227–242.
[11] S.L. Zhong, X.J. Cui, H.L. Cai, T.Z. Fu, C. Zhao, H. Na, Crosslinked sulfonated poly(ether ether ketone) proton exchange membranes for direct methanol fuel cell applications, J. Power Sources 164 (1) (2007) 65–72.
[12] L. Jorissen, V. Gogel, J. Kerres, J. Garche, New membranes for direct methanol fuel cells, J. Power Sources 105 (2) (2002) 267–273.
[13] N. Asano, M. Aoki, S. Suzuki, K. Miyatake, H. Uchida, M. Watanabe, Aliphatic/aromatic polyimide ionomers as a proton conductive membrane for fuel cell applications, J. Amer Chem. Soc. 128 (5) (2006) 1762–1769.
[14] Q.H. Guo, P.N. Pintauro, H. Tang, S. O'Connor, Sulfonated and crosslinked polyphosphazene-based proton-exchange membranes, J. Membr. Sci. 154 (2) (1999) 175–181.
[15] F. Wang, M. Hickner, Y.S. Kim, T.A. Zawodzinski, J.E. McGrath, Direct polymerization of sulfonated poly(arylene ether sulfone) random (statistical) copolymers: candidates for new proton exchange membranes, J. Membr. Sci. 197 (1–2) (2002) 231–242.
[16] S.D. Park, Y.J. Chang, J.C. Jung, W. Lee, H. Chang, H. Kim, In-situ crosslinked polymer electrolyte membranes from thermally reactive oligomers for direct methanol fuel cells, Macromol. Symp. 249–250 (1) (2007) 202–208.
[17] S.C. Gil, J.C. Kim, D. Ahn, J.-S. Jang, H. Kim, J.C. Jung, et al., Thermally crosslinked sulfonated polyethersulfone proton exchange membranes for direct methanol fuel cells, J. Membr. Sci. 417–418 (2012) 2.
[18] N.H. Jalani, Development of Nanocomposite Polymer Electrolyte Membranes for Higher Temperature PEM Fuel Cells, Worcester Polytechnic Institute, 2006. Chem Eng.
[19] L. Barbora, S. Acharya, A. Verma, Synthesis and ex-situ characterization of nafion/TiO2 composite membranes for direct ethanol fuel cell, Macromol. Symp. 277 (1) (2009) 177–189.
[20] C.H. Park, H.K. Kim, C.H. Lee, H.B. Park, Y.M. Lee, Nafion nanocomposite membranes: Effect of fluorosurfactants on hydrophobic silica nanoparticle dispersion and direct methanol fuel cell performance, J. Power Sources 194 (2) (2009) 646–654.
[21] R.V. Gummaraju, R.B. Moore, K.A. Mauritz, Asymmetric [Nafion]/[silicon oxide] hybrid membranes via the in situ sol–gel reaction for tetraethoxysilane, J. Polym. Sci. B Polym. Phys. 34 (1996) 2383–2392.
[22] Z. Liu, Nano-TiO2-coated polymer electrolyte membranes for direct methanol fuel cells, J. Power Sources 157 (1) (2006) 207–211.
[23] G.M. Anilkumar, S. Nakazawa, T. Okubo, T. Yamaguchi, Proton conducting phosphated zirconia-sulfonated polyether sulfone nanohybrid electrolyte for low humidity, wide-temperature PEMFC operation, Electrochem Comm. 8 (1) (2006) 133–136.
[24] S. Ren, G. Sun, C. Li, S. Song, Q. Xin, X. Yang, Sulfated zirconia–Nafion composite membranes for higher temperature direct methanol fuel cells, J. Power Sources 157 (2) (2006) 724–726.
[25] V. Tricoli, F. Nannetti, Zeolite–Nafion composites as ion conducting membrane materials, Electrochim Act. 48 (2003) 2625–2633.
[26] W. Lee, H. Kim, T.K. Kim, H. Chang, Nafion based organic/inorganic composite membrane for air-breathing direct methanol fuel cells, J. Membr. Sci. 292 (1–2) (2007) 29–34.
[27] T.K. Kim, M. Kang, Y.S. Choi, H.K. Kim, W. Lee, H. Chang, Preparation of Nafion-sulfonated clay nanocomposite membrane for direct methanol fuel cells via a film coating process, J. Power Sources 165 (2007) 1–8.
[28] D.-H. Jung, S.Y. Cho, D.H. Peck, D.R. Shin, J.S. Kim, Preparation and performance of a Nafion®/montmorillonite nanocomposite membrane for direct methanol fuel cell, J. Power Sources 118 (2003) 205–211.
[29] M.M. Hasani-Sadrabadi, E. Dashtimoghadam, S.R. Ghaffarian, M.H. Hasani Sadrabadi, M. Heidari, H. Moaddel, Novel high-performance nanocomposite proton exchange membranes based on poly (ether sulfone), Renew. Energy 35 (1) (2009) 226–231.
[30] Y.G. Seo, M.A. Kim, H. Lee, W. Lee, Solution processed thin films of non-aggregated TiO2 nanoparticles prepared by mild solvothermal treatment, Sol. Energy Mater Sol. Cells 95 (1) (2013) 332–335.
[31] E. Scolan, C. Sanchez, Synthesis and Characterization of Surface-Protected Nanocrystalline Titania Particles, Chem. Mater 10 (10) (1998) 3217–3223.
[32] J. Pan, H. Zhang, W. Chen, M. Pan, Nafion–zirconia nanocomposite membranes formed via in situ sol–gel process, Int. J. Hydrogen Energy 35 (2010) 2796–2801.
[33] C.-K. Lin, J.-F. Kuo, C.-Y. Chen, Preparation of nitrated sulfonated poly(ether ether ketone) membranes for reducing methanol permeability in direct methanol fuel cell applications, J. Power Sources 187 (2) (2009) 341–347.
[34] W. Lee, S.C. Gil, H. Lee, H. Kim, Improved Mechanical Strength of Partially Sulfonated Polystyrene-poly (dimethylsiloxane) Block Copolymer Proton Exchange Membranes by Nanoscale Sequestration of Thermally Crosslinked Silicone, Macromol. Res. 17 (6) (2009) 451–454.
[35] E.S. Kwak, W. Lee, N.G. Park, J. Kim, H. Lee, Compact Inverse-Opal Electrode Using Non-Aggregated TiO2 Nanoparticles for Dye-Sensitized Solar Cells, Adv. Func. Mater 19 (7) (2009) 1093–1099.
[36] W.S. Chung, H. Lee, W. Lee, M.J. Ko, N.G. Park, B.K. Ju, et al., Solution processed polymer tandem cell utilizing organic layer coated nano-crystalline TiO2 as interlayer, Org. Electron 11 (4) (2010) 521–528.
[37] K.G. Kanade, J.O. Baeg, S.K. Apte, T.L. Prakash, B.B. Kale, Synthesis and characterization of nanocrystallined zirconia by hydrothermal method, Mater ResBull. 43 (3) (2008) 723–729.
[38] B. Kumar, J.P. Fellner, Polymer-ceramic composite protonic conductors, J. Power Sources 123 (2) (2003) 132–136.
[39] Z. Wu, G. Sun, W. Jin, H. Hou, S. Wang, Q. Xin, Nafion® and nano-size TiO2–SO42– solid superacid composite membrane for direct methanol fuel cell, J. Membr. Sci. 313 (2008) 336–343.
[40] C.H. Rhee, H. Kim, J.S. Lee, H. Chang, Nafion/sulfonated montmorillonite composite: a new concept electrolyte membrane for direct methanol fuel cells, Chem. Mater 17 (2005) 1691–1697.